energy&fuels

pubs.acs.org/EF

Article

Characterization of Asphaltenes and Petroleum Using Benzenepolycarboxylic Acids (BPCAs) and Compound-Specific Stable Carbon Isotopes

Aleksandar I. Goranov, Morgan F. Schaller, Jonathan A. Long, Jr., David C. Podgorski, and Sasha Wagner*

Cite This: https://doi.org/10.1021/acs.energyfuels.1c02374

Read Online

ACCESS | Metrics & More | Article Recommendations | Supporting Information

ABSTRACT: Asphaltenes are unique molecules whose abundance and structure control physicochemical properties of petroleum. The structural appearance of asphaltenes (island versus archipelago architecture) is dependent upon the sample type and petroleum source, but distinguishing between the two architectures remains analytically challenging. Here, we present the application of the benzenepolycarboxylic acid (BPCA) molecular marker method to characterize the condensed aromatic core (ConAC) of asphaltenes. This thermochemolytic technique converts ConAC moieties to benzenehexacarboxylic (B6CA) and benzenepentacarboxylic (B5CA) acids, which are quantified chromatographically and used to estimate the quantity of ConAC in petrogenic samples. Sequential compound-specific isotope analysis (CSIA) with stable carbon isotopes ($\delta^{13}C$) of BPCA markers can provide an additional dimension of characterization relative to carbon source and processing. We analyzed the heavy Maya sour and light Marlin platform (MPCO) crude oils and their respective asphaltene fractions. Quantitative BPCA analysis revealed that Maya sour asphaltenes contained higher quantities of larger ConAC relative to MPCO asphaltenes. CSIA of individual BPCA markers showed that Maya sour asphaltenes are ^{13}C-depleted relative to MPCO asphaltenes, even though bulk organic $\delta^{13}C$ values were similar among sample types. Taken together, the results of quantitative and CSIA BPCA analyses suggest island-dominant architecture for Maya asphaltenes and archipelago-dominant architecture for MPCO asphaltenes. Therefore, BPCA quantification and BPCA-specific $\delta^{13}C$ analysis may be a useful approach characterizing petrogenic samples as well as differentiating between structural architectures of condensed aromatic cores in asphaltenes. This article is in tribute to Dr. Alan G. Marshall for his numerous contributions to the scientific developments in analytical chemistry and environmental science, specifically the co-invention of the Fourier transform ion cyclotron resonance mass spectrometry (FT−ICR−MS) technique and his work toward the deconvolution of complex matrices, such as asphaltenes and petroleum.

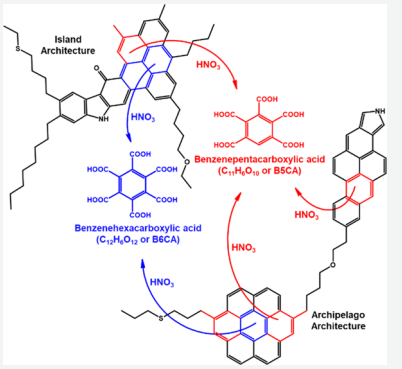

1. INTRODUCTION

Asphaltenes have an extremely high structural diversity and control the physicochemical properties of petroleum.[1−4] The molecular composition of asphaltenes is not well-understood as a result of their operational definition: the fraction of petroleum that is insoluble in *n*-alkanes (typically *n*-pentane or *n*-heptane) and soluble in toluene.[5] Determining how structural characteristics of asphaltenes relate to the physicochemical behavior of crude oil is critical for streamlining the efficiency and effectiveness of both up- and downstream petroleum production operations.[6] Asphaltenes tend to aggregate,[7] which can cause pipeline blockages and lead to production delays and even shutdowns. If not removed from the production process, asphaltenes also reduce the overall petroleum yield and quality. Thus, monitorization and characterization of asphaltenes is a critical analytical endeavor for the petroleum industry.[8]

Asphaltenes are typically isolated from crude oil using preparative-scale chromatography with silica gel, which separates a petroleum sample into four compound fractions: saturated hydrocarbons, aromatic molecules, resinous compounds, and asphaltenes, a technique known as SARA analysis.[9] SARA fractionation has enabled the separation of critical petroleum components for their characterization.[10] Asphaltenes are enriched in nitrogen, sulfur, and oxygen (NSO) relative to other petroleum fractions.[9] NSO compounds are highly polar, tend to retain water, are usually of high molecular weight,[9] and are generally difficult to volatilize and analyze using the classical analytical techniques employed in the petroleum industry (e.g., gas chromatography). Thus,

Special Issue: 2021 Pioneers in Energy Research: Alan Marshall

Received: July 14, 2021
Revised: September 23, 2021

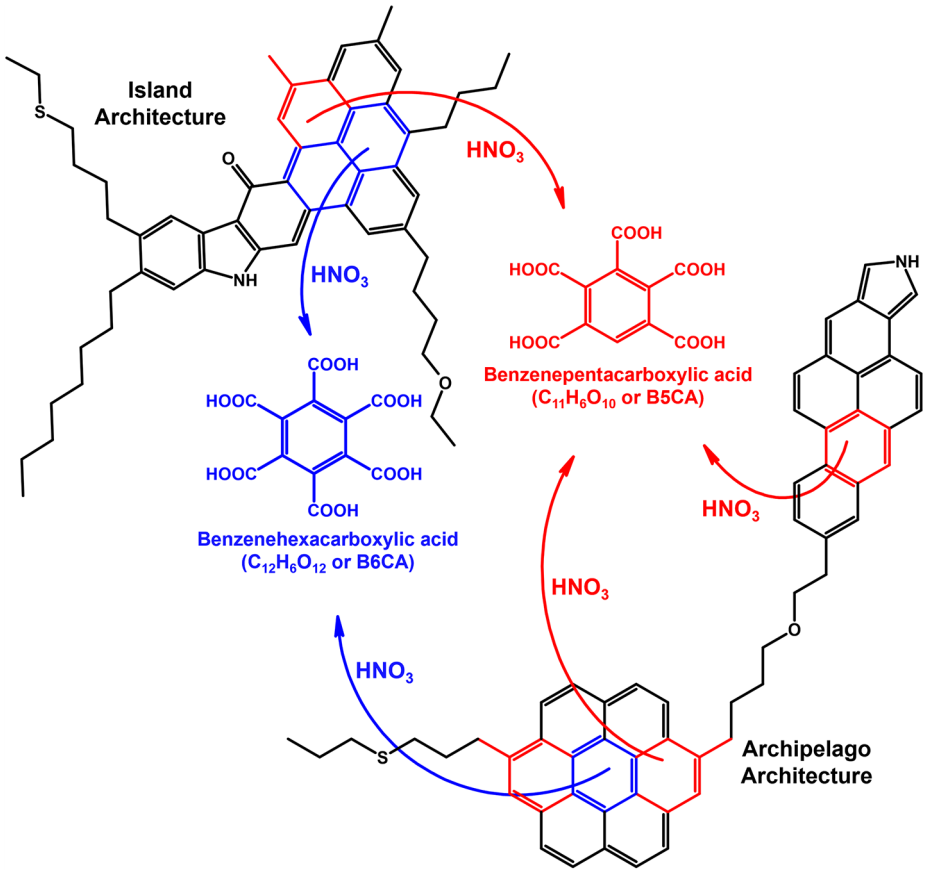

Figure 1. Examples of asphaltene molecules with island and archipelago architectures. Upon nitric acid (HNO_3) oxidation, aromatic rings colored in blue would be converted to benzenehexacarboxylic acid (B6CA) markers, while those colored in red would be converted to benzenepentacarboxylic acid (B5CA) markers. Structures were modified from Kuznicki et al.[27] Note that, while B6CA and B5CA markers may be produced from the same structural moiety, the exact yield of each BPCA marker per asphaltene molecule will depend upon the oxidation patterns that occur.

employment of advanced mass spectrometric or spectroscopic techniques is necessary for the characterization of asphaltenes.[11−15] Despite their high molecular diversity, asphaltenes are broadly classified into two groups based on their structural appearance: "island" and "archipelago".[16] Asphaltene molecules with an archipelago architecture are comprised of several small condensed aromatic groups linked together by aliphatic chains.[17] Asphaltenes with an island architecture (also known as continental architecture) are comprised of a single large condensed aromatic core that is polysubstituted with multiple aliphatic branches (Figure 1).[18] Asphaltene configuration and content are critical controls of the viscosity of crude oil, which can vary by several orders of magnitude.[19,20] Differentiating between island and archipelago architectures enables the optimization of the petroleum source[18] and prediction of connectivity/gradients of crude oils across geologic reservoirs.[21−23] Only recent applications of advanced mass spectrometric techniques (e.g., ultrahigh-resolution mass spectrometry coupled with fragmentation pattern analysis) have made it possible to distinguish among island and archipelago architectures,[1,16,21,23−25] but these methods are neither broadly accessible nor available as benchtop instruments. Thus, differentiation between island and archipelago architectures remains analytically challenging and is largely dependent upon traditional methods, such as pyrolysis − gas chromatography − mass spectrometry.

Here, we demonstrate the utility of benzenepolycarboxylic acid (BPCA) molecular marker analysis for characterizing asphaltenes and petroleum. This method is well-used in the environmental sciences to characterize condensed aromatic compounds on a quantitative carbon basis (i.e., condensed aromatic carbon) in various environmental matrices (commonly termed "black carbon", especially when referring to a pyrogenic source). Collectively, we refer to condensed aromatic compounds/carbon as ConAC, which terminology we also employ here to refer to condensed aromatic cores in asphaltenes. We use ConAC as an overarching term, which includes polycyclic aromatic hydrocarbons (PAHs), oxygenated PAHs, graphite nanotubes, and other substances consisting of condensed aromatic moieties. The BPCA method converts ConAC moieties into BPCA molecular markers upon thermochemolytic digestion with concentrated nitric acid (Figure 1).[28] The BPCA markers range from the highly substituted benzenehexacarboxylic (B6CA) and benzenepentacarboxylic (B5CA) acids to the less substituted benzenedi-, benzenetri-, and benzenetetracarboxylic acids (B2CA, B3CA, and B4CA) and their nitrated derivatives.[29] The BPCA method was originally developed to quantify ConAC in soils[28] and has since been extensively refined for improved sample preparation and robust BPCA marker quantification using chromatographic techniques.[30] The BPCA method described here differs from previous asphaltene structural assessments using ruthenium-ion-catalyzed oxidation (RICO),

https://doi.org/10.1021/acs.energyfuels.1c02374
Energy Fuels XXXX, XXX, XXX−XXX

which transforms most aromatic structures to CO_2 and selectively preserves alkyl groups.[12] Although RICO analysis of ConAC does produce BPCA molecular markers, RICO oxidation products are dominated by the less substituted varieties (B2CA, B3CA, and B4CA) and B5CA and B6CA are produced in far lower quantities than what is theoretically expected.[12] In contrast, the BPCA method described here uses nitric acid oxidation to convert alkyl chains and most monoaromatic moieties to CO_2 and to convert ConAC to BPCA molecular markers.[29,31] Thus, the analytical window of the RICO method selectively preserves and enables the characterization of aliphatic asphaltene moieties, whereas the analytical window of the BPCA method is refined to specifically target ConAC asphaltene moieties. Here, we focus on using B5CA and B6CA molecular markers, which are the dominant products of HNO_3 oxidation of ConAC[32] and are proxies of high specificity for ConAC,[33,34] with no known interferences from non-condensed structures. B5CA and B6CA markers are only produced from carbon-based six-member rings within ConAC structures and will not be produced from smaller rings (e.g., cyclopentyl moieties) or rings with NSO heteroelements (pyridinic, pyranic, and thiopyranic moieties).

Recent adaptations of the BPCA method incorporate compound-specific radiocarbon ($\Delta^{14}C$) and stable carbon ($\delta^{13}C$) isotopic measurements[35−37] to assist in evaluating sources and apparent age of ConAC in the global biogeochemical cycle.[38−41] Environmental ConAC is ubiquitous and derived from both pyrogenic and petrogenic sources,[30,40,42,43] but the biogeochemical dynamics of this long-lived carbon fraction remain poorly constrained. BPCA markers have been identified as a potentially conservative tracer for petroleum ConAC in subterranean oil plumes,[44] but their utility in specifically investigating asphaltenes has not been previously assessed. Additionally, previous studies employing compound-specific isotopic analysis (CSIA) have primarily focused on the isotopic composition of *n*-alkanes released from the asphaltene fraction during pyrolysis.[45,46] Therefore, prior asphaltene CSIA data only reflect the isotopic signatures of alkyl side chains and bridges and, thus, do not provide information on the isotopic composition of ConAC.

In this proof-of-concept study, we evaluated the applicability of BPCA markers and BPCA-specific $\delta^{13}C$ measurements for differentiating between two different crude oils and their asphaltene fractions. We analyzed the heavy Maya sour and light Macondo surrogate (MPCO) crude oils and their respective asphaltenes. These crude oils are compositionally different (Figure S1 of the Supporting Information), which allowed us to assess the utility of BPCA markers for differentiating between island and archipelago architectures. Because the abundance of island- and archipelago-type asphaltenes is dependent upon sample composition and geologic origin,[21−23] we expected BPCA quantities and BPCA-specific $\delta^{13}C$ measurements to differ significantly among petroleum types and asphaltene architectures.

2. EXPERIMENTAL SECTION

2.1. Asphaltene Isolation. Maya sour and Marlin platform (MPCO) crude oils were obtained from Shell Global Solutions and BP (August 2011, chain of custody 20110803-Tarr-072) and used without further purification. Maya crude oil is a sour petroleum produced by Cangrejera Petrochemical Complex (Veracruz, Mexico), with a sulfur content of 3.4 wt.% and American Petroleum Institute (API) gravity of 21.5°.[47] MPCO is a sweet petroleum from the Gulf of Mexico and is chemically identical to the Macondo oil[48] released during the Deepwater Horizon 2010 oil spill.[49] MPCO has a sulfur content of 0.3 wt.% and API gravity of 32.1°.[48,50,51] Asphaltene isolation was performed following standard methods of ASTM International (ASTM D2007-80 and ASTM D6560-12),[52−54] with some modifications as described below.

Crude oil (10 g) and 500 mL of *n*-heptane (99%, Fisher Chemical) were added to a 1000 mL round-bottom flask resulting to a volumetric ratio of 1:50. The mixture was heated to 100 °C and refluxed for one hour. Then, heating was turned off, and the solution awaited cooling while continuing to reflux for an additional 30 minutes. Flasks were capped and stored in the dark overnight, allowing for asphaltenes to aggregate and precipitate. Asphaltenes were isolated by filtration (Whatman 1 filter, 70 mm). Crude oils were extracted in triplicate to obtain three technical replicate asphaltene fractions for each oil. The resultant asphaltenes of the Maya oil were of crystalline form and were ground to fine powders with pre-combusted mortars and pestles. The resultant asphaltenes of MPCO were highly viscous and were used without further treatment. Prior to the analyses described below, asphaltenes and crude oils were quantitatively dissolved in toluene (high-performance liquid chromatography (HPLC) grade, Fisher Chemical). In total, eight samples were analyzed, including the Maya and MPCO crude oils and their three associated asphaltene replicate fractions.

2.2. Bulk Elemental and Isotopic Analysis. Carbon (C%) and nitrogen (N%) contents as well as bulk stable carbon isotopic composition ($\delta^{13}C$) were measured using elemental analysis − isotope-ratio mass spectrometry (EA−IRMS). Asphaltene and crude oil solutions in toluene were aliquoted into tin capsules (5 × 9 mm, CE Elantech), and toluene was evaporated at 60 °C in a programmable oven for 12 hours. Samples were analyzed on an Elementar vario ISOTOPE select elemental analyzer equipped with a thermal conductivity detector and further coupled to an Isoprime 100 IRMS run in continuous flow mode. Carbon and nitrogen contents in weight percent were calculated on the basis of the signal from the thermal conductivity detector, which was externally calibrated against a certified standard of acetanilide (Costech). $\delta^{13}C$ values were computed on the basis of the $^{13}C/^{12}C$ ratio of the sample relative to a pulse of CO_2 reference gas. The obtained $\delta^{13}C$ measurements were corrected against a petroleum-based certified isotopic reference material (NBS 22, $\delta^{13}C = -30.031 \pm 0.043‰$).[55−57] This calibration standard was chosen to match the matrix of the asphaltene fraction and crude oil samples. Isotopic values are expressed relative to Vienna Pee Dee Belemnite (VPDB) on a scale normalized by assigning consensus values of −46.6‰ to lithium carbonate (L-SVEC) and +1.95‰ to calcium carbonate (NBS 19).[55] IRMS performance was evaluated throughout the analytical sequences using a caffeine certified reference material (IAEA 600, $\delta^{13}C = -27.771 \pm 0.043‰$)[55] and an internal (surrogate) laboratory standard of peach leaves (NIST 1547). Analyses were performed in quadruplicate with a typical standard deviation of $\delta^{13}C$ measurements of ≤ 0.04‰. Quantitative C% and N% and isotopic $\delta^{13}C$ data are provided in Table S1 of the Supporting Information and presented in Figure 3 and Figure S1 of the Supporting Information.

2.3. BPCA Quantitative Analysis. Samples dissolved in toluene were transferred to 2 mL glass ampules (Fisher Scientific catalog number 01-215L), and toluene (plus other volatile organics) was evaporated under N_2 flow (AirGas, NI HP300). Then, 0.5 mL of concentrated nitric acid (Fisher Chemical catalog number A200212, Certified ACS Plus grade) was added to the deposited organics, and the ampules were flame-sealed. Thermochemolytic digestion was executed in a programmable oven (ThermoScientific Thermolyne) at 160 °C for 6 hours.[58] Then, ampules were opened, and nitric acid was removed by evaporation in a sand bath (60 °C) under N_2 flow (AirGas, NI HP300). The BPCA-containing digestate was then dissolved in 1 mL of 0.6 M phosphoric acid (Fisher Chemical catalog number A260-500, 85%, HPLC grade) and stored at −20 °C until quantification.[35]

https://doi.org/10.1021/acs.energyfuels.1c02374
Energy Fuels XXXX, XXX, XXX−XXX

Benzenehexacarboxylic acid (B6CA, $C_{12}H_6O_{12}$, Fisher Chemical catalog number B02465G, 98+%) and benzenepentacarboxylic acid (B5CA, $C_{11}H_6O_{10}$, Fisher Chemical catalog number B095225G, 98+%) were quantified using a Thermo Fisher Scientific UltiMate 3000 HPLC system with spectrophotometric detection at 240 nm. Separation was achieved using an Agilent InfinityLab Poroshell 120 Phenyl-Hexyl analytical column (4.6 × 150 mm, 2.7 μm, Agilent catalog number 693975-912) with matching guard filters (Agilent catalog number 820750-914) and organic-free elution conditions as previously described.[35] Exemplary chromatograms of crude oils and asphaltenes are shown in Figure S2 of the Supporting Information. B6CA and B5CA eluted at characteristic times and were quantified using external calibration curves. Other HNO_3 oxidation products, such as less substituted BPCA markers (B2CA, B3CA, and B4CA as well as their nitrated derivatives),[29] are also visible but are neither identified nor quantified as a result of their poor reliability in characterizing ConAC.[33,34,59] Three technical replicates were prepared of each sample and analyzed with a typical relative standard deviation of < 5%. The quantified B6CA and B5CA markers were used to derive the following two parameters:

B6CA:B5CA ratio: the molar ratio of B6CA:B5CA markers produced after nitric acid digestion (eq 1). The ratio has a dimensionless value related to aromatic condensation; i.e., it serves as a proxy for the average number of fused rings of ConAC in asphaltenes.[29,31,60] A higher B6CA:B5CA ratio is indicative of molecules with a higher degree of aromaticity.

$$\text{B6CA: B5CA} = \frac{\text{moles of B6CA produced}}{\text{moles of B5CA produced}} \quad (1)$$

Condensed aromatic carbon (ConAC) content: A quantitative estimate of ConAC derived from the quantified B6CA and B5CA markers. BPCA carbon-equivalents (mg-C) are scaled with a multiplication factor of 7.04[34] to estimate the amount of ConAC (nominator in eq 2) present in the sample before the HNO_3 digestion. ConAC quantity is normalized to the amount of organic carbon used in the HNO_3 digestion by multiplying the sample weight with the carbon content (C%) from EA−IRMS. C-normalized ConAC quantity is expressed in weight percent (eq 2).

$$\text{condensed aromatic carbon (ConAC) content} = \frac{7.04 \times [\text{B6CA (mg-C)} + \text{B5CA (mg-C)}]}{\text{sample weight (mg)} \times \text{C\%}} \times 100 \quad (2)$$

Several conversion factors exist in the literature[28,29,31,32,34,61] to convert from the BPCA marker concentration to the ConAC concentration with no current consensus as to which scaling factor should be used. The conversion factor chosen here (7.04) is developed after a recovery study of graphene oxide (containing 100% ConAC) and assumes a linear relationship between the produced B6CA and B5CA markers from ConAC.[34] The B6CA and B5CA quantities produced during the digestion (milligrams of BPCA-C per milligram of organic carbon) are provided in Table S2 of the Supporting Information; therefore, ConAC quantities may be recalculated as conversion factors continue to be refined.

2.4. Compound-Specific Isotope Analysis (CSIA) of BPCA Markers. Samples used for quantitative BPCA analysis were additionally analyzed on a separate chromatograph for measuring $\delta^{13}C$ values of the B6CA and B5CA markers. A second identical HPLC system (Thermo Fisher Scientific UltiMate 3000), column (Agilent InfinityLab Poroshell 120 Phenyl-Hexyl), and separation conditions were used as described previously in section 2.3. Measurement of $\delta^{13}C$ values of BPCAs was performed using a Delta V ADVANTAGE IRMS detector connected to the HPLC system via a Thermo Fisher Isolink interface.[62] The Isolink interface converts BPCA markers to CO_2 via thermally assisted acidic oxidation with persulfate.[63] Oxidation efficiencies for B5CA and B6CA have been tested and determined to be ≈100% under the described elution and oxidation conditions by Wagner et al.[35] The CO_2 gas is extracted from the liquid eluent using an in-line membrane, and CO_2 is fed into the IRMS detector for measurement of its $^{13}C/^{12}C$ ratio. $\delta^{13}C$ values were computed on the basis of the $^{13}C/^{12}C$ ratio of the sample relative to a pulse of CO_2 reference gas. The obtained $\delta^{13}C$ measurements were corrected against the $\delta^{13}C$ values of the B6CA and B5CA standards, which act as surrogate isotopic standards. Their isotopic values were quantified as described above in section 2.2. Thus, isotopic values are expressed relative to VPDB on a scale normalized by assigning consensus values of −46.6‰ to lithium carbonate (L-SVEC) and +1.95‰ to calcium carbonate (NBS 19).[55] Instrument performance and possible sample carryover were evaluated throughout the analytical sequences by injecting standard and blank samples every 10 samples. Analyses were performed in triplicate with a typical standard deviation of BPCA-specific $\delta^{13}C$ of ≤ 0.12‰. Because BPCA separation and $\delta^{13}C$ measurements were performed using organic-free elution and oxidation conditions, no derivatization or extraneous carbon correction was required. Thus, obtained $\delta^{13}C$ values are true to the BPCA markers, and no further mathematical corrections beyond their calibration to VPDB were necessary. Further details about the analysis, instrumentation, or data treatment have been described in detail by Wagner et al.[35] While the HPLC−IRMS system described here was primarily used for CSIA of BPCA markers, it also provided a quantitative measure of total carbon being oxidized, allowing for quantification of BPCA markers if desired. Quantitative results of the two detection methods (spectroscopic and mass spectrometric) are highly comparable, as shown in Figure S4 of the Supporting Information.

2.5. Statistical Analysis. Differences among means of different observations (B6CA:B5CA ratios, ConAC contents, and $\delta^{13}C$ values) of the eight samples were evaluated using one-way analysis of variance (ANOVA) coupled with Tukey-Kramer post hoc tests in MATLAB using the *anova1* and *multcompare* functions, respectively. Pairs of means were evaluated using a two-sample *t* test using the *ttest2* function. Pearson correlation was performed using the *corrcoef* function. To compare the two different asphaltenes to each other or their parent oils, the observations for the three asphaltene technical replicates were pooled together to result in a sample size of 9 (for BPCA data) or 12 (for EA-IRMS data). All statistical analyses were performed with a confidence level (α) of 95%.

3. RESULTS AND DISCUSSION

3.1. Asphaltene Characterization Using BPCA Quantities. Chromatographic analysis of the oxidized asphaltene and crude oil samples revealed the presence of peaks corresponding to the B6CA and B5CA molecular markers (Figure S2 of the Supporting Information). The formation of these molecules was expected because they have been previously identified in petroleum and coal types of petrogenic samples.[30,42] Here, we found that measured BPCA ratios and corresponding ConAC contents were distinctly different among the Maya sour and MPCO crude oil samples and their associated asphaltene fractions (Figure 2).

The B6CA:B5CA ratio, a proxy for the average number of fused rings of ConAC in asphaltenes, was significantly different among asphaltene fractions and crude oils (Figure 2A). The ratio of Maya crude oil (0.76 ± 0.01) was significantly higher than that of MPCO crude oil (0.52 ± 0.02). The ratios of asphaltene fractions were consistently and significantly higher than ratios of the parent crude oils. The ratio of Maya asphaltene fractions (1.15 ± 0.05) was significantly higher than the ratio of MPCO asphaltene fractions (0.77 ± 0.10). Inconsistencies in B6CA:B5CA ratios observed among same source asphaltene fractions suggest that entrapped maltenes[52,64,65] or other impurities may exist. The range of B6CA:B5CA ratios observed for crude oil and asphaltene fractions (0.50 − 1.24) is similar to the range observed for ConAC in aquatic and terrestrial environments (0.23 −

https://doi.org/10.1021/acs.energyfuels.1c02374
Energy Fuels XXXX, XXX, XXX−XXX

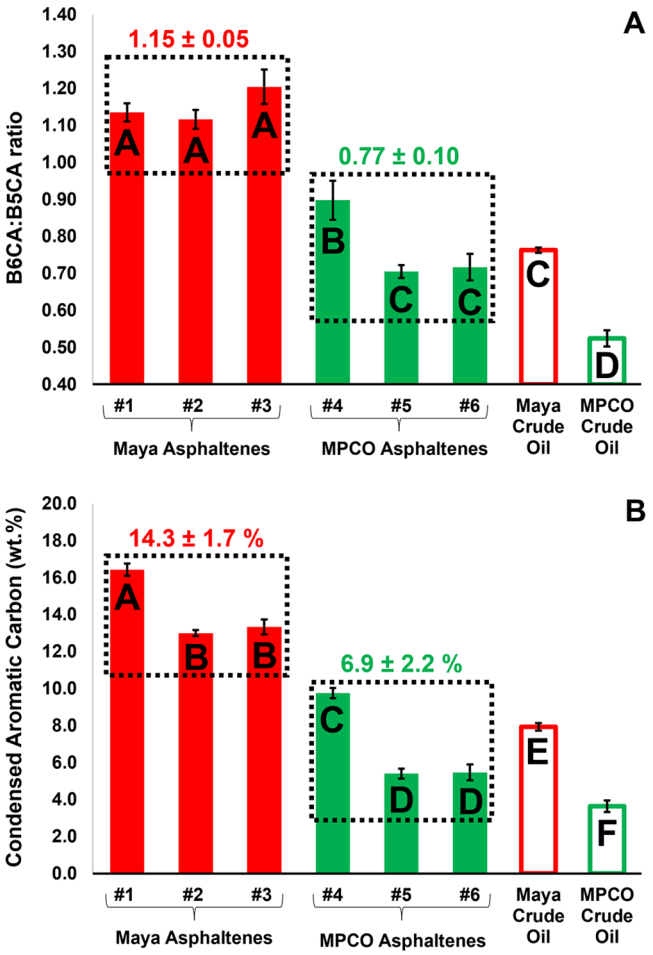

Figure 2. Quantitative benzenepolycarboxylic acid (BPCA) analysis of crude oils and their asphaltene fractions. Panel A corresponds to benzenehexacarboxylic acid (B6CA):benzenepentacarboxylic acid (B5CA) molar ratios indicative of the degree of condensation of the aromatic clusters in the studied samples. Panel B correspond to quantified condensed aromatic carbon in weight percent relative to organic carbon in the studied samples. Standard deviations of triplicate measurements are shown as error bars. Analysis of variance (ANOVA) determined that there is a significant difference ($p < 0.05$) among the means of the eight samples for both measurements. Samples are grouped with black letters based on the statistical similarity of their means as determined by Tukey-Kramer post hoc tests. Samples of the Maya oil are colored in red, while samples of the Marlin platform (MPCO) oil are colored in green. Measurements of asphaltene fractions are denoted with filled bars, while measurements of crude oils are denoted with empty bars. The three replicate asphaltene isolates of each oil are grouped with black dashed boxes, and the mean and standard deviation are shown on top.

1.11).[35] On average, ConAC structures that have been characterized in aquatic and terrestrial environments contain ≈ 7 rings.[66−68] Thus, similarities among aquatic, terrestrial, and petrogenic B6CA:B5CA ratios are expected, because asphaltene ConAC structures generally have 4 − 10 fused rings.[23,69]

The ConAC content of Maya crude oil (7.9 ± 0.2%) was significantly higher than that of MPCO crude oil (3.6 ± 0.3%). The ConAC contents of asphaltene fractions were consistently and significantly higher than the ConAC content of the parent crude oil (Figure 2B). The ConAC content of Maya asphaltene fractions (14.3 ± 1.7%) was significantly higher than the ConAC content of MPCO asphaltene fractions (6.9 ± 2.2%). The employed SARA analysis for the extraction of the asphaltenes can be the source of inconsistency in the ConAC content among same source asphaltene fractions (Figure 2B). Because the ConAC content is expressed on a carbon-basis, observed variability in the asphaltene extraction yield (Figure S1A of the Supporting Information) propagates into the final normalized measurements. The observed variability likely originated from maltene entrapment during the flocculation and precipitation[52,64,65] or because the asphaltenes were not extensively washed to remove vaporizable material.[25]

The observed significant differences among B6CA:B5CA ratios and ConAC contents suggest that the Maya and MPCO asphaltenes are of different structural architectures. Higher B6CA:B5CA ratios and higher ConAC contents observed for Maya asphaltenes (Figure 2) provide support for island-type architecture for this heavy crude oil. In contrast, lower B6CA:B5CA ratios and lower ConAC contents observed for the MPCO asphaltenes suggest that this lighter oil contains archipelago-type asphaltenes. The trends in B6CA:B5CA ratios mirror the measured ConAC contents, indicating that samples of higher aromaticity (with a higher B6CA:B5CA ratio) are also more enriched in ConAC (Pearson correlation; $p < 0.05$; Figure S3 of the Supporting Information). One of the Maya asphaltenes (sample 1) appeared to deviate from the observed correlation, which is likely due to maltenes or other unwashed vaporizable impurities affecting the normalization of ConAC quantity to total carbon. Collectively, these results indicate that the Maya crude oil and its associated asphaltene fractions have larger proportions of more condensed ConAC than the MPCO crude oil and its associated asphaltene fractions. For both oil types, the asphaltene fractions were enriched in higher quantities of ConAC than the parent crude, which suggests the presence of a higher number of fused aromatic rings in asphaltene fractions overall. These observations parallel decades of research on observed higher aromaticity of asphaltene fractions relative to their parent crude oils.[26]

3.2. Asphaltene Characterization Using BPCA Compound-Specific Isotope Analysis (CSIA). To contextualize BPCA-specific isotopic data, bulk $\delta^{13}C$ values of crude oil samples and associated asphaltene fractions were also measured (Figure 3A). Maya crude (−27.76 ± 0.06 ‰) was significantly ^{13}C-enriched compared to MPCO crude oil (−27.94 ± 0.05 ‰), suggesting different carbon sources or biogeochemical/hydrothermal processing.[70,71] However, bulk $\delta^{13}C$ values for the Maya and MPCO asphaltene fractions (−27.78 ± 0.06 ‰ and −27.62 ± 0.26 ‰, respectively) were statistically similar. These data suggest that bulk $\delta^{13}C$ analysis of asphaltene fractions may not be a reliable indicator of asphaltene structural architectures among diverse crude oil types.

By conducting BPCA-specific $\delta^{13}C$ analysis, we can probe the carbon source of ConAC moieties in asphaltenes and whole crude oils. BPCA-specific $\delta^{13}C$ measurements have enabled the tracking and source apportionment of ConAC in various aquatic systems,[38,39] but no such work has been previously conducted on petroleum or its sub-components. Previous research using CSIA of PAHs has shown that larger (i.e., more condensed) PAHs exhibit lower (i.e., ^{13}C-depleted) $\delta^{13}C$ values relative to smaller (i.e., less condensed) PAHs.[72,73] This relationship appears to be largely driven by the extent of oil maturation[72] and allows us to hypothesize that that carbon

https://doi.org/10.1021/acs.energyfuels.1c02374
Energy Fuels XXXX, XXX, XXX−XXX

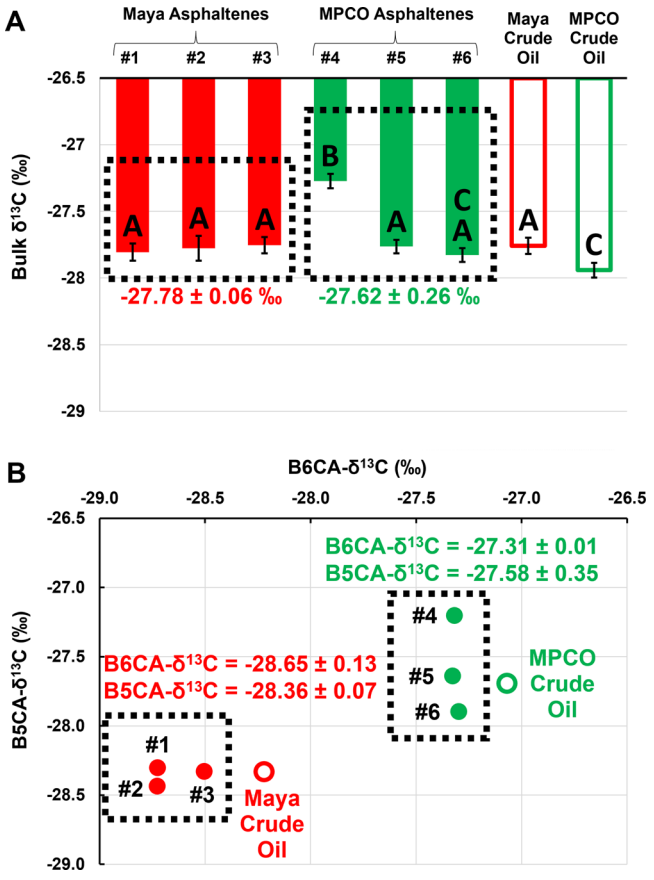

Figure 3. Isotopic data for asphaltene fractions and crude oils. Panel A corresponds to bulk $\delta^{13}C$ measurements. Standard deviations of quadruplicate measurements are shown as error bars. Analysis of variance (ANOVA) determined that there is a significant difference ($p < 0.05$) among the means of the eight samples. Samples are grouped with black letters based on the statistical similarity of their means determined by Tukey-Kramer post hoc tests. Panel B corresponds to compound-specific $\delta^{13}C$ measurements of benzenepolycarboxylic acid markers: benzenehexacarboxylic acid (B6CA-$\delta^{13}C$) versus benzenepentacarboxylic acid (B5CA-$\delta^{13}C$). Samples of the Maya oil are colored in red, while samples of the Marlin platform (MPCO) oil are colored in green. Measurements of asphaltene fractions are denoted with filled bars (panel A) or filled markers (panel B), while measurements of crude oils are denoted with empty bars (panel A) or empty markers (panel B). The three replicate asphaltene isolates of each oil are grouped with black dashed boxes, and the mean and standard deviation are shown on top.

in more condensed island architectures should be ^{13}C-depleted relative to carbon in less condensed archipelago architectures. BPCA-specific $\delta^{13}C$ analysis revealed that ConAC in Maya asphaltene fractions (B6CA-$\delta^{13}C$ = −28.22 ± 0.06 ‰, and B5CA-$\delta^{13}C$ = −28.33 ± 0.21 ‰) was significantly ^{13}C-depleted compared to ConAC in MPCO asphaltene fractions (B6CA-$\delta^{13}C$ = −27.07 ± 0.15 ‰, and B5CA-$\delta^{13}C$ = −27.69 ± 0.02 ‰). These results confirm our hypothesis and suggest that BPCA-specific $\delta^{13}C$ analysis can be used as another dimension of differentiation between asphaltene structural architectures in heavy and light crude oil types.

Asphaltenes produce different quantities of B6CA and B5CA based on the size and structural constituents of their ConAC moieties. B5CA markers are typically produced when peripheral aromatic rings are oxidized, whereas B6CA markers are formed when completely substituted aromatic rings are oxidized[29] (Figure 1). The carboxyl groups of BPCA are not only produced from fused ring structures but also originate from aromatic structures with functional groups (e.g., CH_3) that would, upon HNO_3 oxidation, be converted to carboxyl groups (COOH). Therefore, B5CA markers may contain isotopic remnants in their carboxyl groups originating from alkyl chains or other peripheral constituents that were formed in biological reactions. In contrast, B6CA markers are primarily derived from ConAC moieties that are internal in ConAC and are therefore physically protected from isotopic modification by biota. Although we have not tested this hypothesis directly, this may explain isotopic offsets observed between B6CA-$\delta^{13}C$ and B5CA-$\delta^{13}C$ values here (Figure 3B) and provide some insight into post-depositional biological alterations of asphaltene isotopic composition.

The average B6CA-$\delta^{13}C$ values of asphaltene isolates (B6CA-$\delta^{13}C$ = −28.65 ± 0.13 ‰ for Maya, and B6CA-$\delta^{13}C$ = −27.31 ± 0.01 ‰ for MPCO) revealed that asphaltene ConAC producing B6CA markers are significantly ^{13}C-depleted than their parent crude oils (B6CA-$\delta^{13}C$ = −28.22 ± 0.06 ‰ for Maya, and B6CA-$\delta^{13}C$ = −27.07 ± 0.15 ‰ for MPCO). This is likely because crude oils are primarily comprised of saturated hydrocarbons, which are highly labile toward biodegradation.[74] If biological reactions occur over the time of petroleum maturation, they will ^{13}C-enrich these aliphatic molecules, which would result in increasing the bulk $\delta^{13}C$ values of the crude oil. ConAC, on the other hand, is resistant to biodegradation,[44,75] and relative to the whole oils, the BPCA-specific $\delta^{13}C$ values remain mostly unaltered by biota.[76]

In contrast with trends from B6CA-$\delta^{13}C$ data, the average B5CA-$\delta^{13}C$ values of asphaltene isolates (B5CA-$\delta^{13}C$ = −28.36 ± 0.07 ‰ for Maya, and B5CA-$\delta^{13}C$ = −27.58 ± 0.35 ‰ for MPCO) revealed that asphaltene ConAC producing B5CA markers is of a statistically similar stable carbon isotopic composition to their parent crude oils (B5CA-$\delta^{13}C$ = −28.33 ± 0.21 ‰ for Maya, and B5CA-$\delta^{13}C$ = −27.69 ± 0.02 ‰ for MPCO). This similarity in carbon signatures is indicative of a similar source and homogenization of peripheral carbon in asphaltenes. We hypothesize that microbially influenced molecules (i.e., ^{13}C-enriched) could influence peripheral functional groups (aliphatic chains) of asphaltene molecules to result in the observed similarity among bulk $\delta^{13}C$ and B5CA-$\delta^{13}C$ values.

The $\delta^{13}C$ values of B6CA and B5CA are significantly correlated in terrestrial aquatic systems[38,39] because they are derived from a similar biomass source and undergo similar environmental processing during riverine export. On the other hand, this correlation has been observed to be insignificant in oceanic systems,[39] indicative of either different sources of ConAC that produce B6CA and B5CA markers or an unsurveyed isotopic fractionation process. Here, we do not have sufficient data along a compositional or geologic gradient to do a similar correlational assessment, but our preliminary data show that a correlation between BPCA-specific $\delta^{13}C$ values for petroleum and asphaltenes may hold true given their terrestrial isotopic signature. This is also expected given that ConAC that produces B6CA and B5CA markers originates from a similar carbon source and/or underwent similar diagenetic processing and isotopic fractionation during the geologic formation of petroleum and associated asphaltenes. Taken together, these data demonstrate the potential utility of BPCA-specific $\delta^{13}C$ measurements in constraining source,

https://doi.org/10.1021/acs.energyfuels.1c02374
Energy Fuels XXXX, XXX, XXX−XXX

structure, and/or geologic history of petroleum and its asphaltene fractions.

3.3. Analytical Considerations and Potential Artifacts.

3.3.1. Benefits and Limitations of Current Analytical Protocols and BPCA-Specific $\delta^{13}C$ Knowledge. Our results show that BPCA markers can be employed to quantify ConAC in asphaltene samples and assess its degree of aromatic condensation. The obtained ConAC content and B6CA:B5CA ratio measurements are shown here to be potentially useful in distinguishing among archipelago and island asphaltene architectures. The quantitative BPCA method is relatively simple and analytically robust and can have a high throughput of 100+ samples a week. It does not require any specialized equipment beyond a temperature-controlled oven and a chromatograph with an autosampler and a spectrophotometric detector. As a result of the high specificity of the BPCA method toward condensed molecules, the method can be employed to characterize ConAC in crude oils and differentiate oils with different sources and/or geologic history without the necessity to perform SARA fractionation. The BPCA method has the potential to greatly streamline analytical assessments in both both up- and downstream petroleum production operations. It must be noted that, for proper calculation of ConAC contents, bulk organic carbon quantification must be performed using elemental analysis or other means. However, bulk organic carbon quantity is not needed for computing the B6CA:B5CA ratio, the parameter that is directly related to the degree of condensation of asphaltene ConAC.

A significant limitation of the BPCA method at present is the uncertain accuracy with which produced BPCAs truly represent quantities of native ConAC in environmental samples. For example, the quantified ConAC content in the asphaltenes of Maya crude is 14.3% (Figure 2B), while analyses using nuclear magnetic resonance have estimated an aromatic content of ∼50%.[77,78] The quantified ConAC content using BPCAs relies upon a scaling factor that has not been previously tested on petrogenic samples. Thus, the BPCA method is only able to estimate the absolute quantity of ConAC as a result of the use of an empirical conversion factor. Another limination of the BPCA method is that condensed NSO-containing rings do not produce B6CA or B5CA markers, which may result in underestimation of ConAC. Future work is needed to fully calibrate the BPCA methodology against a variety of certified samples with known ConAC content as well as with samples enriched in NSO functionalities. However, even though the absolute quantity of the ConAC content may appear to be underestimated, on relative terms, the ConAC content still has the utility to differentiate among different asphaltene architectures (Figure 2B).

In contrast with the quantitative BPCA approach performed on a HPLC system with a spectrophotometric detector, the HPLC−IRMS system is highly specialized and does not permit for quick and routine CSIA of BPCAs. Employing CSIA, however, has been immensely useful in enhancing the knowledge about sources of ConAC within the global biogeochemical cycles in surficial environmental systems.[38,39] Because CSIA BPCA methodologies are relatively recent,[35,37] our knowledge and availability of BPCA $\delta^{13}C$ data are still limited. However, our data (Figure 3B) clearly shows that the CSIA BPCA method has a high utility in the characterization of asphaltenes and petroleum and may allow for differentiating between asphaltene architectures upon further investigation.

3.3.2. Gas-Chromatography-Based BPCA Methods and Considerations. While we have employed a HPLC-based BPCA method[35] in this study, we recognize that gas chromatography (GC) is a more common analytical technique for the characterization of petroleum and its fractions. Most of the BPCA quantification methods, including the very first method by Glaser et al.,[28] in fact employ gas chromatography and are refined to suit diverse suites of samples (see Table 1 in the study by Chang et al.[30] for a summary of methods). GC-based BPCA methodologies, however, are of a higher level of complexity relative to the HPLC approaches. A very clean matrix is required for GC-based analysis, complicating the protocol with additional sample preparation steps (sample demineralization, filtration, and cation exchange).[79] Furthermore, as a result of their high oxygen content, BPCA molecules are not volatile. Their separation and quantification using gas chromatographic systems are not possible without derivatization using (trimethylsilyl)diazomethane[29] or other agents. The employment of GC-based methods also requires the use of more standards, and the calibration is of higher complexity.[80] A direct method comparison found that GC-based methods underestimate the ConAC content 1.5 times more than HPLC-based methods,[79] indicative of the many additional sources of error when GC approaches are used.

Performing CSIA using GC methods is even more problematic as a result of the alteration of the BPCA-$\delta^{13}C$ signatures from extraneous carbon from the derivatization agent. This would require a specialized isotope correction,[81] additionally increasing the uncertainties associated with the $\delta^{13}C$ measurements.

3.3.3. Effect of Maltene and Vaporizable Material Occlusions in Asphaltene Isolates. Apparent outliers in the B6CA:B5CA ratios and ConAC contents of Maya and MPCO asphaltene isolates (Figures 2 and 3) may be explained by occlusion of maltenes or vaporizable material in the asphaltene fractions. Maltenes are NSO *n*-heptane-soluble substances that contain lower proportions of ConAC with a lower number of fused rings.[10] In a petroleum matrix, asphaltene molecules are stabilized by maltenes via interactions based on steric guest-host mechanisms or intermolecular attractions, such as π-π stacking.[82,83] Thus, during asphaltene isolation, maltene impurities may remain occluded inside asphaltene aggregates.[52,64,65] If asphaltenes are not properly purified using solvent washes during the extraction process, vaporizable material may also remain occluded[25] and affect the BPCA measurements and normalization. The occlusion of maltenes and vaporizable material will result in the underestimation of ConAC contents and B6CA:B5CA ratios. This is because maltenes contain less and smaller ConAC than asphaltenes,[10] and the unwashed vaporizable material is likely poor in ConAC but contributes to an enriched organic carbon measurement used in the ConAC content normalization. The occlusion of maltenes and vaporizable material has likely contributed to the observed variability in the quantitative measurements of the technical replicate asphaltene fractions of the two oils (Figure 2 and Figure S1 of the Supporting Information).

One of the asphaltene isolates of the MPCO crude oil (asphaltene 4) was an apparent outlier in the isotopic data (Figure 3). B5CA markers derived from this asphaltene fraction were ^{13}C-enriched relative to other MPCO technical replicate fractions (Figure 3B). Bulk $\delta^{13}C$ measurements also indicated that asphaltene 4 was ^{13}C-enriched compared to other fractions (Figure 3A). Previous studies using isotope

https://doi.org/10.1021/acs.energyfuels.1c02374
Energy Fuels XXXX, XXX, XXX−XXX

analysis of maltenes have primarily focused on the CSIA of *n*-alkanes released from the maltene fraction during pyrolysis.[84] Maltenes are generally more ^{13}C-enriched than asphaltenes, which strongly suggests that asphaltene 4 has signifficant maltene occlusions. Occlusion of vaporizable material enriched in ^{13}C may also be contributing to the outlying measurements of asphaltene 4. Asphaltene extractions in future work should employ a more robust extraction protocol[25,52] and aim to characterize the BPCA signatures of maltene and vaporizable material fractions. This will allow us to distinguish between the quantitative and isotopic BPCA signatures in asphaltenes with occuled impurities and prevent erroneous interpretations.

3.4. Environmental Implications and Future Recommendations. Aromatization reactions that occur during combustion and hydrothermal processes do not fractionate (alter) $\delta^{13}C$ composition.[85] Furthermore, ConAC is resistant to biogeochemical alteration in the environment[44,75] and does not undergo isotopic fractionation during controlled biodegradation experiments on short time scales.[76] However, isotopic offsets in BPCA-specific $\delta^{13}C$ values among environmental samples can vary up to 8 ‰ depending upon the source and organic carbon fraction.[35,39] This suggests that BPCA-specific $\delta^{13}C$ measurements may be used to differentiate between ConAC sources within and among environmental reservoirs. Similarly, if we assume the $\delta^{13}C$ composition of asphaltene-derived BPCAs to remain faithful to their original carbon source, then BPCA CSIA may facilitate the development of robust constraints on asphaltene source and geologic formation conditions.

Asphaltene characterization and architecture differentiation are significant analytical challenges in the petroleum industry. The preliminary results presented here demonstrate that quantitative (ConAC content and B6CA:B5CA ratio) and isotopic (BPCA-specific $\delta^{13}C$ values) measurements can potentially address the challenge of differentiation between archipelago- and island-dominated asphaltene fractions of crude oils. Employment of the BPCA method would allow for constraining sources and/or geologic history of crude oils by specifically targeting their asphaltene fractions. However, the present study cannot conclude that the BPCA method can confidently differentiate among asphaltene architectures. It is possible that both the Maya crude and MPCO asphaltenes are of the same architecture but have different parameters (B6CA:B5CA ratio, ConAC content, and BPCA-specific isotopic signatures). There is some expected variability among parameters within the same architecture, and it is possible that the observed different parameters for the two asphaltenes, although significantly different, are still within the variability of one type of architecture. Further work is needed to assess the utility of the BPCA method across a large suite of samples as well as to properly determine a threshold that separates the island and archipelago architectures. Additionally, future research should seek to investigate how to distinguish between asphaltene and maltene signatures in the BPCA data. To achieve these goals, it is necessary to evaluate a diverse set of asphaltenes, maltenes, and their crude oil counterparts across gradients of API gravities and sulfur contents. This would allow for establishing B6CA:B5CA ratio and $\delta^{13}C$ value thresholds for the distinction between island versus archipelago structural architectures. Evaluating a larger suite of petrogenic materials will also allow for the development of a robust scaling factor for converting measured BPCA quantities to accurate ConAC contents in petroleum and its asphaltene fractions.

The quantitative and isotopic characterization of ConAC in petroleum and/or associated asphaltene fractions could also assist in answering persistent questions regarding the global biogeochemical cycling of ConAC in surficial environmental systems. For example, ConAC comprises ∼2% of dissolved organic carbon in global oceans,[86,87] yet the source of this long-lived carbon component remains enigmatic.[39] Petroleum-derived ConAC can enter the deep ocean via oil seeps.[88] Hydrothermal vents have also been suggested as a potential source of ConAC,[66] graphite,[89] or other refractory forms of carbon[90,91] to the open ocean. Given its resistance to biodegradation,[44,75,76] ConAC preferentially accumulates in petroleum and other natural reservoirs, including oceanic environments.[92] Our preliminary results suggest that the stable carbon isotopic signature of petrogenic ConAC (≈ −28‰;Figure 3) is terrestrial-like, which is dissimilar to the observed marine-like oceanic signature of oceanic ConAC ($\delta^{13}C \approx -23$ ‰).[39] However, further work is needed to establish whether hydrothermal ConAC emitted via marine seeps and/or hydrothermal venting systems is isotopically comparable to the crude oils and ConAC-rich asphaltene fractions analyzed here.

4. CONCLUSION

In this proof-of-concept study, the application of BPCA markers on Maya and MPCO crude oils and their asphaltene fractions revealed that BPCA quantities (translated into the B6CA:B5CA ratio and ConAC content) and stable carbon isotopic composition ($\delta^{13}C$) can successfully determine the quantity and relative size and assess the source of condensed aromatic cores in asphaltenes and petroleum. Clear differences in the data suggest that a possible threshold exists that could enable differentiation among island and archipelago structural architectures of asphaltenes. Application of BPCA markers may be an important approach for optimizing up- and downstream processing and increasing economic value. However, future research is needed to robustly test the application of BPCA markers on oils with diverse API gravities and sulfur contents and evaluate their asphaltene fractions. This work is necessary for robustly assessing the ability of the BPCA method to distinguish among island and archipelago asphaltene architectures across diverse crude oil sources.

■ ASSOCIATED CONTENT

Supporting Information

The Supporting Information is available free of charge at https://pubs.acs.org/doi/10.1021/acs.energyfuels.1c02374.

Quantitative (C% and N%) and bulk $\delta^{13}C$ data from EA−IRMS, HPLC chromatograms, numeric data from the quantitative BPCA approach (BPCA quantities, ratios, and ConAC quantities), Pearson correlation among ConAC quantities and B6CA:B5CA ratios, comparison of BPCA results obtained from HPLC coupled with different detectors (spectrophotometer versus IRMS), and numeric data from CSIA of BPCAs (BPCA-specific $\delta^{13}C$ data) (PDF)

■ AUTHOR INFORMATION

Corresponding Author

Sasha Wagner − *Department of Earth and Environmental Sciences, Rensselaer Polytechnic Institute, Troy, New York 12180, United States*; Email: wagnes3@rpi.edu

https://doi.org/10.1021/acs.energyfuels.1c02374
Energy Fuels XXXX, XXX, XXX−XXX

Authors

Aleksandar I. Goranov − *Department of Earth and Environmental Sciences, Rensselaer Polytechnic Institute, Troy, New York 12180, United States;* orcid.org/0000-0002-5103-0838

Morgan F. Schaller − *Department of Earth and Environmental Sciences, Rensselaer Polytechnic Institute, Troy, New York 12180, United States*

Jonathan A. Long, Jr. − *Department of Chemistry, University of New Orleans, New Orleans, Louisiana 70148, United States*

David C. Podgorski − *Department of Chemistry and Pontchartrain Institute for Environmental Sciences, Chemical Analysis & Mass Spectrometry Facility, Shea Penland Coastal Education and Research Facility, University of New Orleans, New Orleans, Louisiana 70148, United States;* orcid.org/0000-0002-1070-5923

Complete contact information is available at: https://pubs.acs.org/10.1021/acs.energyfuels.1c02374

Notes

The authors declare no competing financial interest.

■ ACKNOWLEDGMENTS

The authors thank Shell Global Solutions and Dr. Matthew A. Tarr for access to the crude oils. This project was funded by the National Science Foundation (Division of Chemical Oceanography, Award OCE 2017577) and the Louisiana Board of Regents Research Competitiveness Subaward. Lastly, the authors express their thankfulness to the Editor-in-Chief Professor Hongwei Wu and two anonymous reviewers for their time and feedback in improving this manuscript.

■ REFERENCES

(1) Chacón-Patiño, M. L.; Rowland, S. M.; Rodgers, R. P. Advances in asphaltene petroleomics. Part 2: Selective separation method that reveals fractions enriched in island and archipelago structural motifs by mass spectrometry. *Energy Fuels* **2018**, *32* (1), 314−328.

(2) Herod, A. A. Limitations of mass spectrometric methods for the characterization of polydisperse materials. *Rapid Commun. Mass Spectrom.* **2010**, *24* (17), 2507−2519.

(3) Purcell, J. M.; Merdrignac, I.; Rodgers, R. P.; Marshall, A. G.; Gauthier, T.; Guibard, I. Stepwise structural characterization of asphaltenes during deep hydroconversion processes determined by atmospheric pressure photoionization (APPI) Fourier transform ion cyclotron resonance (FT-ICR) mass spectrometry. *Energy Fuels* **2010**, *24* (4), 2257−2265.

(4) Herod, A. A.; Bartle, K. D.; Morgan, T. J.; Kandiyoti, R. Analytical methods for characterizing high-mass complex polydisperse hydrocarbon mixtures: An overview. *Chem. Rev.* **2012**, *112* (7), 3892−3923.

(5) Fan, T.; Buckley, J. S. Rapid and accurate SARA analysis of medium gravity crude oils. *Energy Fuels* **2002**, *16* (6), 1571−1575.

(6) Akbarzadeh, K.; Hammami, A.; Kharrat, A.; Zhang, D. Asphaltenes—Problematic but Rich in Potential. *Oilfield Rev.* **2007**, *19* (2), 22−43.

(7) McKenna, A. M.; Donald, L. J.; Fitzsimmons, J. E.; Juyal, P.; Spicer, V.; Standing, K. G.; Marshall, A. G.; Rodgers, R. P. Heavy petroleum composition. 3. Asphaltene aggregation. *Energy Fuels* **2013**, *27* (3), 1246−1256.

(8) Alimohammadi, S.; Zendehboudi, S.; James, L. A comprehensive review of asphaltene deposition in petroleum reservoirs: Theory, challenges, and tips. *Fuel* **2019**, *252*, 753−791.

(9) Jewell, D. M.; Weber, J. H.; Bunger, J. W.; Plancher, H.; Latham, D. R. Ion-exchange, coordination, and adsorption chromatographic separation of heavy-end petroleum distillates. *Anal. Chem.* **1972**, *44* (8), 1391−1395.

(10) Gaspar, A.; Zellermann, E.; Lababidi, S.; Reece, J.; Schrader, W. Characterization of saturates, aromatics, resins, and asphaltenes heavy crude oil fractions by atmospheric pressure laser ionization Fourier transform ion cyclotron resonance mass spectrometry. *Energy Fuels* **2012**, *26* (6), 3481−3487.

(11) Buenrostro-Gonzalez, E.; Groenzin, H.; Lira-Galeana, C.; Mullins, O. C. The overriding chemical principles that define asphaltenes. *Energy Fuels* **2001**, *15* (4), 972−978.

(12) Strausz, O. P.; Mojelsky, T. W.; Lown, E. M. The molecular structure of asphaltene: An unfolding story. *Fuel* **1992**, *71* (12), 1355−1363.

(13) Tang, W.; Hurt, M. R.; Sheng, H.; Riedeman, J. S.; Borton, D. J.; Slater, P.; Kenttämaa, H. I. Structural comparison of asphaltenes of different origins using multi-stage tandem mass spectrometry. *Energy Fuels* **2015**, *29* (3), 1309−1314.

(14) Hosseini-Dastgerdi, Z.; Tabatabaei-Nejad, S. A. R.; Khodapanah, E.; Sahraei, E. A comprehensive study on mechanism of formation and techniques to diagnose asphaltene structure; molecular and aggregates: A review. *Asia-Pac. J. Chem. Eng.* **2015**, *10* (1), 1−14.

(15) Rueda-Velásquez, R. I.; Freund, H.; Qian, K.; Olmstead, W. N.; Gray, M. R. Characterization of asphaltene building blocks by cracking under favorable hydrogenation conditions. *Energy Fuels* **2013**, *27* (4), 1817−1829.

(16) Chacón-Patiño, M. L.; Rowland, S. M.; Rodgers, R. P. Advances in asphaltene petroleomics. Part 1: Asphaltenes are composed of abundant island and archipelago structural motifs. *Energy Fuels* **2017**, *31* (12), 13509−13518.

(17) Alvarez-Ramírez, F.; Ruiz-Morales, Y. Island versus archipelago architecture for asphaltenes: Polycyclic aromatic hydrocarbon dimer theoretical studies. *Energy Fuels* **2013**, *27* (4), 1791−1808.

(18) Mullins, O. C. Petroleomics and structure-function relations of crude oils and asphaltenes. In *Asphaltenes, Heavy Oils, and Petroleomics*; Mullins, O. C., Sheu, E. Y., Hammami, A., Marshall, A. G., Eds.; Springer: New York, 2007; pp 1−16, DOI: 10.1007/0-387-68903-6_1.

(19) Lin, M. S.; Lunsford, K. M.; Glover, C. J.; Davison, R. R.; Bullin, J. A. The effects of asphaltenes on the chemical and physical characteristics of asphalt. In *Asphaltenes: Fundamentals and Applications*; Sheu, E. Y., Mullins, O. C., Eds.; Springer: Boston, MA, 1995; pp 155−176, DOI: 10.1007/978-1-4757-9293-5_5.

(20) Sirota, E. B.; Lin, M. Y. Physical behavior of asphaltenes. *Energy Fuels* **2007**, *21* (5), 2809−2815.

(21) Chacón-Patiño, M. L.; Rowland, S. M.; Rodgers, R. P. Advances in asphaltene petroleomics. Part 3. Dominance of island or archipelago structural motif is sample dependent. *Energy Fuels* **2018**, *32* (9), 9106−9120.

(22) McKenna, A. M.; Chacón-Patiño, M. L.; Weisbrod, C. R.; Blakney, G. T.; Rodgers, R. P. Molecular-level characterization of asphaltenes isolated from distillation cuts. *Energy Fuels* **2019**, *33* (3), 2018−2029.

(23) Neumann, A.; Chacón-Patiño, M. L.; Rodgers, R. P.; Rüger, C. P.; Zimmermann, R. Investigation of Island/Single-Core- and Archipelago/Multicore-Enriched Asphaltenes and Their Solubility Fractions by Thermal Analysis Coupled with High-Resolution Fourier Transform Ion Cyclotron Resonance Mass Spectrometry. *Energy Fuels* **2021**, *35* (5), 3808−3824.

(24) Podgorski, D. C.; Corilo, Y. E.; Nyadong, L.; Lobodin, V. V.; Bythell, B. J.; Robbins, W. K.; McKenna, A. M.; Marshall, A. G.; Rodgers, R. P. Heavy petroleum composition. 5. Compositional and structural continuum of petroleum revealed. *Energy Fuels* **2013**, *27* (3), 1268−1276.

(25) Rüger, C. P.; Grimmer, C.; Sklorz, M.; Neumann, A.; Streibel, T.; Zimmermann, R. Combination of Different Thermal Analysis Methods Coupled to Mass Spectrometry for the Analysis of Asphaltenes and Their Parent Crude Oils: Comprehensive Character-

ization of the Molecular Pyrolysis Pattern. *Energy Fuels* **2018**, *32* (3), 2699−2711.
(26) Fakher, S.; Ahdaya, M.; Elturki, M.; Imqam, A. Critical review of asphaltene properties and factors impacting its stability in crude oil. *J. Pet. Explor. Prod. Technol.* **2020**, *10* (3), 1183−1200.
(27) Kuznicki, T.; Masliyah, J. H.; Bhattacharjee, S. Molecular dynamics study of model molecules resembling asphaltene-like structures in aqueous organic solvent systems. *Energy Fuels* **2008**, *22* (4), 2379−2389.
(28) Glaser, B.; Haumaier, L.; Guggenberger, G.; Zech, W. Black carbon in soils: The use of benzenecarboxylic acids as specific markers. *Org. Geochem.* **1998**, *29* (4), 811−819.
(29) Ziolkowski, L. A.; Chamberlin, A. R.; Greaves, J.; Druffel, E. R. M. Quantification of black carbon in marine systems using the benzene polycarboxylic acid method: A mechanistic and yield study. *Limnol. Oceanogr.: Methods* **2011**, *9* (4), 140−140.
(30) Chang, Z.; Tian, L.; Li, F.; Zhou, Y.; Wu, M.; Steinberg, C. E. W.; Dong, X.; Pan, B.; Xing, B. Benzene polycarboxylic acid—A useful marker for condensed organic matter, but not for only pyrogenic black carbon. *Sci. Total Environ.* **2018**, *626*, 660−667.
(31) Dittmar, T. The molecular level determination of black carbon in marine dissolved organic matter. *Org. Geochem.* **2008**, *39* (4), 396−407.
(32) Stubbins, A.; Spencer, R. G. M.; Mann, P. J.; Holmes, R. M.; McClelland, J. W.; Niggemann, J.; Dittmar, T. Utilizing colored dissolved organic matter to derive dissolved black carbon export by Arctic rivers. *Front. Earth Sci.* **2015**, *3*, 63.
(33) Kappenberg, A.; Bläsing, M.; Lehndorff, E.; Amelung, W. Black carbon assessment using benzene polycarboxylic acids: Limitations for organic-rich matrices. *Org. Geochem.* **2016**, *94*, 47−51.
(34) Bostick, K. W.; Zimmerman, A. R.; Wozniak, A. S.; Mitra, S.; Hatcher, P. G. Production and composition of pyrogenic dissolved organic matter from a logical series of laboratory-generated chars. *Front. Earth Sci.* **2018**, *6*, 43.
(35) Wagner, S.; Brandes, J.; Goranov, A. I.; Drake, T. W.; Spencer, R. G. M.; Stubbins, A. Online quantification and compound-specific stable isotopic analysis of black carbon in environmental matrices via liquid chromatography-isotope ratio mass spectrometry. *Limnol. Oceanogr.: Methods* **2017**, *15* (12), 995−1006.
(36) Hanke, U. M.; Wacker, L.; Haghipour, N.; Schmidt, M. W. I.; Eglinton, T. I.; McIntyre, C. P. Comprehensive radiocarbon analysis of benzene polycarboxylic acids (BPCAs) derived from pyrogenic carbon in environmental samples. *Radiocarbon* **2017**, *59* (4), 1103−1116.
(37) Wiedemeier, D. B.; Lang, S. Q.; Gierga, M.; Abiven, S.; Bernasconi, S. M.; Früh-Green, G. L.; Hajdas, I.; Hanke, U. M.; Hilf, M. D.; McIntyre, C. P.; Scheider, M. P. W.; Smittenberg, R. H.; Wacker, L.; Wiesenberg, G. L. B.; Schmidt, M. W. I. Characterization, quantification and compound-specific isotopic analysis of pyrogenic carbon using benzene polycarboxylic acids (BPCA). *J. Visualized Exp.* **2016**, *111*, e53922.
(38) Drake, T. W.; Wagner, S.; Stubbins, A.; Wabakanghanzi, J. N.; Dinga, J. B.; Six, J.; Spencer, R. G. M. Du feu à l'eau: Source and flux of dissolved black carbon from the Congo River. *Global Biogeochem. Cycles* **2020**, *34* (8), e2020GB006560.
(39) Wagner, S.; Brandes, J.; Spencer, R. G. M.; Ma, K.; Rosengard, S. Z.; Moura, J. M. S.; Stubbins, A. Isotopic composition of oceanic dissolved black carbon reveals non-riverine source. *Nat. Commun.* **2019**, *10* (1), 5064.
(40) Coppola, A. I.; Wiedemeier, D. B.; Galy, V.; Haghipour, N.; Hanke, U. M.; Nascimento, G. S.; Usman, M.; Blattmann, T. M.; Reisser, M.; Freymond, C. V.; Zhao, M.; Voss, B.; Wacker, L.; Schefuß, E.; Peucker-Ehrenbrink, B.; Abiven, S.; Schmidt, M. W. I.; Eglinton, T. I. Global-scale evidence for the refractory nature of riverine black carbon. *Nat. Geosci.* **2018**, *11* (8), 584−588.
(41) Coppola, A. I.; Seidel, M.; Ward, N. D.; Viviroli, D.; Nascimento, G. S.; Haghipour, N.; Revels, B. N.; Abiven, S.; Jones, M. W.; Richey, J. E.; Eglinton, T. I.; Dittmar, T.; Schmidt, M. W. I. Marked isotopic variability within and between the Amazon River and marine dissolved black carbon pools. *Nat. Commun.* **2019**, *10* (1), 4018.
(42) Hindersmann, B.; Achten, C. Accelerated benzene polycarboxylic acid analysis by liquid chromatography-time-of-flight-mass spectrometry for the determination of petrogenic and pyrogenic carbon. *Journal of Chromatography A* **2017**, *1510*, 57−65.
(43) Wagner, S.; Jaffé, R.; Stubbins, A. Dissolved black carbon in aquatic ecosystems. *Limnology and Oceanography Letters* **2018**, *3* (3), 168−185.
(44) Podgorski, D. C.; Zito, P.; Kellerman, A. M.; Bekins, B. A.; Cozzarelli, I. M.; Smith, D. F.; Cao, X.; Schmidt-Rohr, K.; Wagner, S.; Stubbins, A.; Spencer, R. G. M. Hydrocarbons to carboxyl-rich alicyclic molecules: A continuum model to describe biodegradation of petroleum-derived dissolved organic matter in contaminated groundwater plumes. *J. Hazard. Mater.* **2021**, *402*, 123998.
(45) Wilhelms, A.; Larter, S. R.; Hall, K. A comparative study of the stable carbon isotopic composition of crude oil alkanes and associated crude oil asphaltene pyrolysate alkanes. *Org. Geochem.* **1994**, *21* (6), 751−760.
(46) Odden, W.; Barth, T.; Talbot, M. R. Compound-specific carbon isotope analysis of natural and artificially generated hydrocarbons in source rocks and petroleum fluids from offshore Mid-Norway. *Org. Geochem.* **2002**, *33* (1), 47−65.
(47) Manriguez, L.; Moreno, A.; Anaya, C. G. Assays for important Mexican crudes updated. *Oil Gas J.* **1991**, *89* (9), 1991.
(48) Worton, D. R.; Zhang, H.; Isaacman-VanWertz, G.; Chan, A. W. H.; Wilson, K. R.; Goldstein, A. H. Comprehensive chemical characterization of hydrocarbons in NIST Standard Reference Material 2779 Gulf of Mexico Crude Oil. *Environ. Sci. Technol.* **2015**, *49* (22), 13130−13138.
(49) Kujawinski, E. B.; Reddy, C. M.; Rodgers, R. P.; Thrash, J. C.; Valentine, D. L.; White, H. K. The first decade of scientific insights from the Deepwater Horizon oil release. *Nature Reviews Earth & Environment* **2020**, *1*, 237−250.
(50) Passow, U.; Sweet, J.; Francis, S.; Xu, C.; Dissanayake, A.; Lin, Y.; Santschi, P.; Quigg, A. Incorporation of oil into diatom aggregates. *Mar. Ecol.: Prog. Ser.* **2019**, *612*, 65−86.
(51) Pelz, O.; Brown, J.; Huddleston, M.; Rand, G.; Gardinali, P.; Stubblefield, W.; BenKinney, M.; Ahnell, A. Selection of a Surrogate MC252 Oil as a Reference Material for Future Aquatic Toxicity Tests and Other Studies. *Proceedings of the SETAC North America 32nd Annual Meeting*; Boston, MA, Nov 13−17, 2011.
(52) Chacón-Patiño, M. L.; Vesga-Martínez, S. J.; Blanco-Tirado, C.; Orrego-Ruiz, J. A.; Gómez-Escudero, A.; Combariza, M. Y. Exploring occluded compounds and their interactions with asphaltene networks using high-resolution mass spectrometry. *Energy Fuels* **2016**, *30* (6), 4550−4561.
(53) ASTM International. *ASTM D6560-12, Standard Test Method for Determination of Asphaltenes (Heptane Insolubles) in Crude Petroleum and Petroleum Products*; ASTM International: West Conshohocken, PA, 2012; pp 1−6, DOI: 10.1520/D6560-12.
(54) ASTM International. *ASTM D2007-80, Standard Test Method for Characteristic Groups in Rubber Extender and Processing Oils and Other Petroleum-Derived Oils by the Clay-Gel Absorption Chromatographic Method*; ASTM International: West Conshohocken, PA, 2007.
(55) Coplen, T. B.; Brand, W. A.; Gehre, M.; Gröning, M.; Meijer, H. A. J.; Toman, B.; Verkouteren, R. M. New guidelines for $\delta^{13}C$ measurements. *Anal. Chem.* **2006**, *78* (7), 2439−2441.
(56) Silverman, S. R. Investigations of petroleum origin and evolution mechanisms by carbon isotope studies. In *Isotopic and Cosmic Chemistry*; Craig, H., Miller, S. L., Wasserburg, G. J., Eds.; North-Holland Publishing Company: Amsterdam, Netherlands, 1964; pp 92−102.
(57) Qi, H.; Coplen, T. B.; Geilmann, H.; Brand, W. A.; Böhlke, J. K. Two new organic reference materials for $\delta^{13}C$ and $\delta^{15}N$ measurements and a new value for the $\delta^{13}C$ of NBS 22 oil. *Rapid Commun. Mass Spectrom.* **2003**, *17* (22), 2483−2487.

https://doi.org/10.1021/acs.energyfuels.1c02374
Energy Fuels XXXX, XXX, XXX−XXX

(58) Ding, Y.; Yamashita, Y.; Dodds, W. K.; Jaffé, R. Dissolved black carbon in grassland streams: Is there an effect of recent fire history? *Chemosphere* **2013**, *90* (10), 2557−2562.
(59) Stubbins, A.; Niggemann, J.; Dittmar, T. Photo-lability of deep ocean dissolved black carbon. *Biogeosciences* **2012**, *9* (5), 1661−1670.
(60) Brodowski, S.; Rodionov, A.; Haumaier, L.; Glaser, B.; Amelung, W. Revised black carbon assessment using benzene polycarboxylic acids. *Org. Geochem.* **2005**, *36* (9), 1299−1310.
(61) Fang, Y.; Chen, Y.; Huang, G.; Hu, L.; Tian, C.; Xie, J.; Lin, J.; Lin, T. Particulate and dissolved black carbon in coastal China seas: Spatiotemporal variations, dynamics, and potential implications. *Environ. Sci. Technol.* **2021**, *55*, 788−796.
(62) Krummen, M.; Hilkert, A. W.; Juchelka, D.; Duhr, A.; Schlüter, H.-J.; Pesch, R. A new concept for isotope ratio monitoring liquid chromatography/mass spectrometry. *Rapid Commun. Mass Spectrom.* **2004**, *18* (19), 2260−2266.
(63) House, D. A. Kinetics and mechanism of oxidations by peroxydisulfate. *Chem. Rev.* **1962**, *62* (3), 185−203.
(64) Liao, Z.; Zhou, H.; Graciaa, A.; Chrostowska, A.; Creux, P.; Geng, A. Adsorption/occlusion characteristics of asphaltenes: Some implication for asphaltene structural features. *Energy Fuels* **2005**, *19* (1), 180−186.
(65) Duran, J. A.; Casas, Y. A.; Xiang, L.; Zhang, L.; Zeng, H.; Yarranton, H. W. Nature of asphaltene aggregates. *Energy Fuels* **2019**, *33* (5), 3694−3710.
(66) Dittmar, T.; Koch, B. P. Thermogenic organic matter dissolved in the abyssal ocean. *Mar. Chem.* **2006**, *102* (3−4), 208−217.
(67) Hockaday, W. C.; Grannas, A. M.; Kim, S.; Hatcher, P. G. The transformation and mobility of charcoal in a fire-impacted watershed. *Geochim. Cosmochim. Acta* **2007**, *71* (14), 3432−3445.
(68) Mao, J. D.; Johnson, R. L.; Lehmann, J.; Olk, D. C.; Neves, E. G.; Thompson, M. L.; Schmidt-Rohr, K. Abundant and stable char residues in soils: Implications for soil fertility and carbon sequestration. *Environ. Sci. Technol.* **2012**, *46* (17), 9571−9576.
(69) Mullins, O. C. The asphaltenes. *Annu. Rev. Anal. Chem.* **2011**, *4* (1), 393−418.
(70) Andrusevich, V. E.; Engel, M. H.; Zumberge, J. E.; Brothers, L. A. Secular, episodic changes in stable carbon isotope composition of crude oils. *Chem. Geol.* **1998**, *152* (1), 59−72.
(71) Sun, Y.; Chen, Z.; Xu, S.; Cai, P. Stable carbon and hydrogen isotopic fractionation of individual n-alkanes accompanying biodegradation: Evidence from a group of progressively biodegraded oils. *Org. Geochem.* **2005**, *36* (2), 225−238.
(72) Clayton, C. J.; Bjorøy, M. Effect of maturity on $^{13}C/^{12}C$ ratios of individual compounds in North Sea oils. *Org. Geochem.* **1994**, *21* (6), 737−750.
(73) Williford, K. H.; Grice, K.; Logan, G. A.; Chen, J.; Huston, D. The molecular and isotopic effects of hydrothermal alteration of organic matter in the Paleoproterozoic McArthur River Pb/Zn/Ag ore deposit. *Earth Planet. Sci. Lett.* **2011**, *301* (1), 382−392.
(74) Oudot, J. Rates of microbial degradation of petroleum components as determined by computerized capillary gas chromatography and computerized mass spectrometry. *Mar. Environ. Res.* **1984**, *13* (4), 277−302.
(75) Bostick, K. W.; Zimmerman, A. R.; Goranov, A. I.; Mitra, S.; Hatcher, P. G.; Wozniak, A. S. Biolability of fresh and photodegraded pyrogenic dissolved organic matter from laboratory-prepared chars. *J. Geophys. Res.: Biogeosci.* **2021**, *126* (5), e2020JG005981.
(76) Mazeas, L.; Budzinski, H.; Raymond, N. Absence of stable carbon isotope fractionation of saturated and polycyclic aromatic hydrocarbons during aerobic bacterial biodegradation. *Org. Geochem.* **2002**, *33* (11), 1259−1272.
(77) Douda, J.; Alvarez, R.; Navarrete Bolaños, J. Characterization of Maya asphaltene and maltene by means of pyrolysis application. *Energy Fuels* **2008**, *22* (4), 2619−2628.
(78) Morgan, T. J.; Alvarez-Rodriguez, P.; George, A.; Herod, A. A.; Kandiyoti, R. Characterization of Maya crude oil maltenes and asphaltenes in terms of structural parameters calculated from nuclear magnetic resonance (NMR) spectroscopy and laser desorption−mass spectroscopy (LD−MS). *Energy Fuels* **2010**, *24* (7), 3977−3989.
(79) Schneider, M. P. W.; Smittenberg, R. H.; Dittmar, T.; Schmidt, M. W. I. Comparison of gas with liquid chromatography for the determination of benzenepolycarboxylic acids as molecular tracers of black carbon. *Org. Geochem.* **2011**, *42* (3), 275−282.
(80) Schneider, M. P. W.; Hilf, M.; Vogt, U. F.; Schmidt, M. W. I. The benzene polycarboxylic acid (BPCA) pattern of wood pyrolyzed between 200 and 1000 °C. *Org. Geochem.* **2010**, *41* (10), 1082−1088.
(81) Gross, S.; Glaser, B. Minimization of carbon addition during derivatization of monosaccharides for compound-specific $\delta^{13}C$ analysis in environmental research. *Rapid Commun. Mass Spectrom.* **2004**, *18* (22), 2753−2764.
(82) Ganeeva, Y. M.; Barskaya, E. E.; Okhotnikova, E. S.; Yusupova, T. N. Features of the composition of compounds trapped in asphaltenes of oils and bitumens of the Bavly oil field. *Energy Fuels* **2021**, *35* (3), 2493−2505.
(83) León, O.; Contreras, E.; Rogel, E.; Dambakli, G.; Espidel, J.; Acevedo, S. The influence of the adsorption of amphiphiles and resins in controlling asphaltene flocculation. *Energy Fuels* **2001**, *15* (5), 1028−1032.
(84) Jia, W.; Chen, S.; Zhu, X.; Peng, P. a.; Xiao, Z. D/H ratio analysis of pyrolysis-released n-alkanes from asphaltenes for correlating oils from different sources. *J. Anal. Appl. Pyrolysis* **2017**, *126*, 99−104.
(85) Holman, A. I.; Grice, K. $\delta^{13}C$ of aromatic compounds in sediments, oils and atmospheric emissions: A review. *Org. Geochem.* **2018**, *123*, 27−37.
(86) Dittmar, T.; Paeng, J. A heat-induced molecular signature in marine dissolved organic matter. *Nat. Geosci.* **2009**, *2* (3), 175−179.
(87) Coppola, A. I.; Druffel, E. R. M. Cycling of black carbon in the ocean. *Geophys. Res. Lett.* **2016**, *43* (9), 4477−4482.
(88) Kvenvolden, K. A.; Cooper, C. K. Natural seepage of crude oil into the marine environment. *Geo-Mar. Lett.* **2003**, *23* (3), 140−146.
(89) Estes, E. R.; Berti, D.; Coffey, N. R.; Hochella, M. F.; Wozniak, A. S.; Luther, G. W. Abiotic synthesis of graphite in hydrothermal vents. *Nat. Commun.* **2019**, *10* (1), 5179.
(90) Druffel, E. R. M.; Griffin, S.; Lewis, C. B.; Rudresh, M.; Garcia, N. G.; Key, R. M.; McNichol, A. P.; Hauksson, N. E.; Walker, B. D. Dissolved organic radiocarbon in the Eastern Pacific and Southern Oceans. *Geophys. Res. Lett.* **2021**, *48* (10), e2021GL092904.
(91) Luther, G. W., III Hydrothermal vents are a source of old refractory organic carbon to the deep ocean. *Geophys. Res. Lett.* **2021**, *48* (17), e2021GL094869.
(92) Valentine, D. L.; Reddy, C. M.; Farwell, C.; Hill, T. M.; Pizarro, O.; Yoerger, D. R.; Camilli, R.; Nelson, R. K.; Peacock, E. E.; Bagby, S. C.; Clarke, B. A.; Roman, C. N.; Soloway, M. Asphalt volcanoes as a potential source of methane to late Pleistocene coastal waters. *Nat. Geosci.* **2010**, *3* (5), 345−348.

https://doi.org/10.1021/acs.energyfuels.1c02374
Energy Fuels XXXX, XXX, XXX−XXX